Influence of the growth direction on properties of ferroelectric ultrathin films

I. Ponomareva* and L. Bellaiche†
Department of Physics, University of Arkansas, Fayetteville, Arkansas 72701, USA
(Received 26 June 2006; published 3 August 2006)

A first-principles-based approach is developed and used to investigate $Pb(Zr_{0.4}Ti_{0.6})O_3$ ultrathin films having different growth directions and subject to different boundary conditions. A wide variety of dipole patterns is found, including ferroelectric phases absent in the bulk and different periodic stripe nanodomains. Moreover, a large enhancement of dielectricity is found in ultrathin films exhibiting a growth direction that differs from a possible direction of the polarization in the corresponding bulk. A set of two general and simple rules is provided to analyze and understand all these features.

DOI: 10.1103/PhysRevB.74.064102 PACS number(s): 77.84.Dy, 68.55.−a, 77.22.Ej, 77.80.Bh

I. INTRODUCTION

Ferroelectric thin films are of high interest[1–12] because of their potential applications in miniaturized devices. Many of their features, such as the dependence of their dipole patterns on boundary conditions and size thickness, are now rather well established.[4–8,11] However, an overwhelming majority of past studies focused on films grown along [001]. As a result, the influence of the *growth direction* on their properties is poorly understood. For instance, Ref. 13 observed that $Pb(Zr_{1-x}Ti_x)O_3$ films surprisingly adopt different macroscopic ferroelectric phases when changing the growth direction from [001] to [111]. Similarly, Ref. 14 revealed that $Pb(Zr_{0.35}Ti_{0.65})O_3$ thin films grown along [111] exhibit, below a certain thickness, a ferroelectric phase differing from the one of the bulk. Reference 15 further reports 90° domains in $PbZr_{0.25}Ti_{0.75}O_3$ film grown along [111], which strikingly differs from the 180° domains discovered in [001] $PbTiO_3$ films.[5] Furthermore, some experiments indicated that properties—such as fatigue endurance and piezoelectricity—can be improved when using a growth direction different from [001]. The microscopic reasons behind such puzzling effects are unknown. The situation is even worse for *ultrathin* films because we are not aware of any work studying the effect of growth direction on their properties, despite their promises to yield unusual phenomena, such as a critical thickness below which ferroelectricity can disappear[4] or the appearance of stripe domains with a remarkably small period.[5]

The aim of this paper is twofold: (i) to demonstrate, via the development and use of a first-principles-based approach, that the growth direction in ferroelectric ultrathin films can lead to original features, such as an enhancement of dielectric responses or different complex dipole patterns, and (ii) to analyze and understand such features via the formulation of two simple rules.

This article is organized as follows. Section II describes the theoretical method we developed and used to tackle the two items indicated above. Section III reports our predictions for different electrical and mechanical boundary conditions, as well as for different films' thickness. Finally, Sec. IV provides a brief summary.

II. METHODOLOGY

We theoretically study thin films made of $Pb(Zr_{0.4}Ti_{0.6})O_3$ (PZT), for which the bulk polarization points along ⟨001⟩ and which lies *outside* the morphotropic phase boundary[16,17] (to prevent the dipoles from easily rotating). Our qualitative predictions should thus also apply to $PbTiO_3$ films. We investigate three common[5,13–15,18,19] growth orientations: namely, [001], [110], and [111]. The films all have Pb-O-terminated surfaces and are represented by supercells that are *finite* along the growth direction, to be denoted as the z' direction, and repeated periodically along two in-plane x' and y' directions. The total energy is written as $\mathcal{E}_{Heff}(\mathbf{p}_i, \mathbf{v}_i, \eta, \sigma_i) + \beta\Sigma_i\langle\mathbf{E}_{dep}\rangle\cdot\mathbf{p}_i$, where $\mathbf{p}_i$ is the local dipole at site i of the supercell and $\mathbf{v}_i$ are inhomogeneous-strain-related variables around this site i. η is the homogeneous strain tensor while σ_i represents the alloy atomic configuration[16]—which is randomly chosen. The expression and first-principles-derived parameters of $\mathcal{E}_{Heff}$ are those given in Refs. 16 and 20 for PZT *bulk*, except for the dipole-dipole interactions for which the expressions derived in Ref. 21 for two-dimensional (2D) nanostructures *under ideal open-circuit conditions* are used. Such conditions naturally lead to a maximum depolarizing field (denoted by $\langle\mathbf{E}_{dep}\rangle$) inside the film when the dipoles point along the growth direction. We mimic a *screening* of $\langle\mathbf{E}_{dep}\rangle$ via the β coefficient. More precisely, the residual depolarizing field has a magnitude equal to $(1-\beta)\ |\langle\mathbf{E}_{dep}\rangle|$. In other words, $\beta=1$ and $\beta=0$ correspond to ideal short-circuit (SC) and open circuit (OC) electrical boundary conditions, respectively, while a value of β in between corresponds to a more realistic situation.[4] Technically, $\langle\mathbf{E}_{dep}\rangle$ is calculated via the atomistic approach of Ref. 22. Different *mechanical* boundary conditions are also simulated thanks to the homogeneous strain η.[7,23] For example, during the simulation associated with an epitaxial strain in the (x',y') planes, four components of η—in the $x'y'z'$ coordinate system—are kept fixed (namely, $\eta_{x'y'}=\eta_{y'x'}=0$ and $\eta_{x'x'}=\eta_{y'y'}=\delta$, with δ characterizing the lattice mismatch between PZT and a chosen substrate) while the other components relax. On the other hand, *all* the components of the strain tensor are allowed to relax for *stress-free* systems. [Note that we do not consider any strain *gradient* mostly because we do not anticipate (based on experimental evidence[5]) that such effect should occur for the films' thicknesses considered here.]

The novelty of our approach with respect to the numerical scheme of Refs. 16 and 20 mostly lies in the fact that the atomic sites' coordinates, the matrices appearing in the

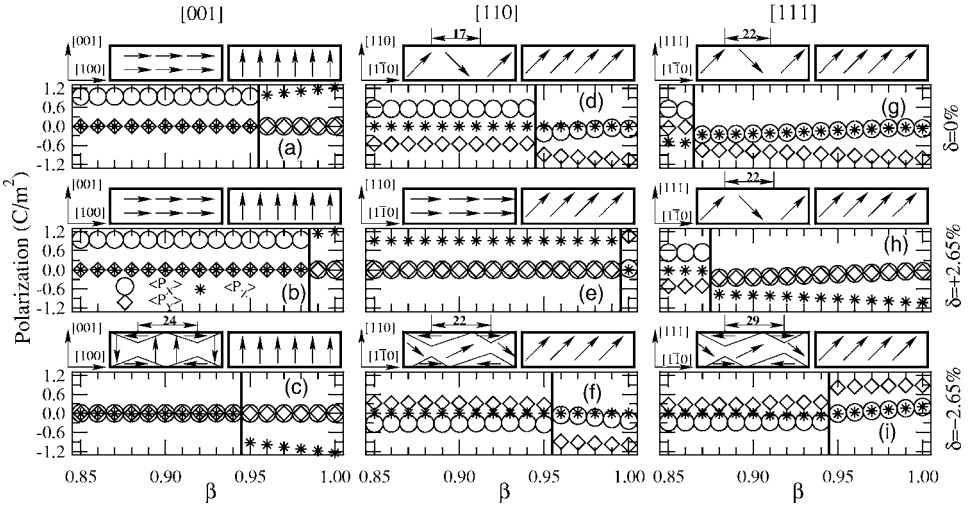

FIG. 1. Cartesian components of the ground-state spontaneous polarization in $Pb(Zr_{0.4}Ti_{0.6})O_3$ (≃46–48-Å-thick) films as a function of the screening coefficient β and expressed in the xyz coordinate system, when choosing 16 and 24 unit cells for the periodicity of the (in-plane) x' and y' directions for [110] and [111] films under compressive strain and 12 unit cells for the periodicity of the x' and y' directions for all other films (see text for the definition of the xyz and $x'y'z'$ coordinate systems). Parts (a), (b), and (c): [001] films under stress free, 2.65% tensile strain, and −2.65% compressive strain, respectively. Parts (d)–(f): same as parts (a)–(c) but for a [110] film. Parts (g)–(i): same as parts (a)–(c) but for a [111] film. The vertical lines characterize the transition of the dipoles pattern from SC-like conditions to OC-like conditions. The schematization of these two different patterns is given above each part. The width of the stripe domains is given in Å.

dipole-dipole interactions,[22] and the strain tensor are all first expressed in the $x'y'z'$ coordinate system and then transformed into the xyz system (in which the x, y, and z axes are along the [100], [010], and [001] directions, respectively) before using the total energy in a Monte Carlo simulation.

III. RESULTS

Figure 1 shows the x, y, and z components of the spontaneous polarization for our PZT thin films at 10 K, as a function of β. Parts (a), (b), and (c) correspond to [001] films under stress-free conditions, a tensile strain of 2.65% in the (x',y') planes, and under a compressive strain of −2.65% in the (x',y') planes, respectively. Parts (d)–(f) and (g)–(i) show similar data but for a growth direction along [110] and [111], respectively. The thicknesses of the [001], [110], and [111] films are equal to 48.0, 48.1, and 46.2 Å, respectively. One can clearly see a broad variety of dipole pattern, which (as we will see) can be understood thanks to the two following simple rules.

Rule 1: Close to SC conditions, the films are *homogeneously* polarized with the polarization **P** being given by

$$\mathbf{P} = \lambda_1 \mathbf{e}_g + \lambda_2 \mathbf{e}_b, \tag{1}$$

where $\mathbf{e}_g$ is the unit vector along the growth direction while $\mathbf{e}_b$ is the unit vector along the direction of the polarization in the corresponding *bulk* that is the *closest* one to $\mathbf{e}_g$. λ_1 and λ_2 are scalars that depend on the material, the epitaxial strain δ, the magnitude of the depolarizing field, and the growth direction. Rule 1 expresses the simultaneous desires of the films to enhance their polarization component along the growth direction for SC-like conditions [first term of Eq. (1)]—in order to reduce short-range energy costs near the surfaces[11]—*and* to have a polarization similar to the bulk [second term of Eq. (1)].

Rule 2: For OC-like conditions, the films adopt patterns for which the out-of-plane component of the spontaneous polarization vanishes, in order to fight against the large depolarizing field associated with such boundary conditions.

Let us now discuss all the studied cases in view of these two rules.

A. Films under ideal SC conditions: Rule 1

Rule 1 can be applied to *stress-free* $Pb(Zr_{0.4}Ti_{0.6})O_3$ films that are under ideal SC and grown along [001] by substituting both $\mathbf{e}_g$ and $\mathbf{e}_b$ by $\mathbf{z}$ in Eq. (1) [Here, $\mathbf{x}$, $\mathbf{y}$, and $\mathbf{z}$ are the unit vectors along the x, y, and z axes, respectively]. As a result, $\mathbf{P}=(\lambda_1+\lambda_2)\mathbf{z}$. The resulting phase is thus tetragonal with a polarization pointing along the growth direction [see Fig. 1(a)], as consistent with measurement.[2] The most interesting cases for ideal SC conditions occur when the growth direction does *not* coincide with any possible direction for the spontaneous polarization of the bulk: Equation (1) implies that such cases lead to a polarization *moving away* from a possible polarization direction in the bulk and thus generate macroscopic phases that do not exist in the corresponding bulk. For instance, our simulations shown in Fig. 1(d) for the stress-free [110] film under ideal SC can be analyzed by choosing $\mathbf{e}_g=-\frac{(\mathbf{x}+\mathbf{y})}{\sqrt{2}}$ and $\mathbf{e}_b=-\mathbf{y}$ in Eq. (1). The resulting **P** is thus $-\frac{\lambda_1}{\sqrt{2}}\mathbf{x}-\left(\frac{\lambda_1}{\sqrt{2}}+\lambda_2\right)\mathbf{y}$, which correspond to the so-called monoclinic M_C phase.[24] [Note that the polarization in the [110] stress-free $Pb(Zr_{0.4}Ti_{0.6})O_3$ film with $\beta=1$ has an equal probability to be $-\frac{\lambda_1}{\sqrt{2}}\mathbf{x}-\left(\frac{\lambda_1}{\sqrt{2}}+\lambda_2\right)\mathbf{y}$ or $+\frac{\lambda_1}{\sqrt{2}}\mathbf{x}+\left(\frac{\lambda_1}{\sqrt{2}}+\lambda_2\right)\mathbf{y}$]. Similarly, the ground state of the stress-free [111] film under per-

TABLE I. Properties of $Pb(Zr_{0.4}Ti_{0.6})O_3$ ($\simeq$46–48-Å-thick) films under ideal SC conditions at $T=10$ K. δ characterizes the epitaxial strain in the (x',y') planes, and $[XYZ]$ is the growth direction. θ_1 is the angle between the polarization in the film and the growth direction while θ_2 is the angle between the polarization in the film and the closest possible direction for the polarization in the bulk. ϵ_{11}, ϵ_{22}, and ϵ_{33} are dielectric coefficients expressed in the orthonormal $x'y'z'$ coordinate system, for which the index "3" refers to the growth direction. The last column shows the corresponding macroscopic phases, with T, M_C, and M_A denoting tetragonal, monoclinic M_C, and monoclinic M_A phases, respectively.

δ	$[XYZ]$	θ_1	θ_2	ϵ_{33}	$\frac{\epsilon_{11}+\epsilon_{22}}{2}$	Phase
0.0	[001]	0.0	0.0	27	44	T
0.0	[110]	40.4	4.6	47	68	M_C
0.0	[111]	49.3	5.4	60	74	M_A
2.65	[001]	0.0	0.0	27	52	T
2.65	[110]	42.7	2.3	41	59	M_C
2.65	[111]	52.0	2.7	58	58	M_A
−2.65	[001]	0.0	0.0	32	36	T
−2.65	[110]	31.7	13.3	45	83	M_C
−2.65	[111]	36.3	18.5	57	122	M_A

fect SC is not tetragonal but rather monoclinic M_A,[24] since its polarization can be written as $-\frac{\lambda_1}{\sqrt{3}}\mathbf{x}-\frac{\lambda_1}{\sqrt{3}}\mathbf{y}-\left(\frac{\lambda_1}{\sqrt{3}}+\lambda_2\right)\mathbf{z}$, resulting from choosing $\mathbf{e}_g=-\frac{(\mathbf{x}+\mathbf{y}+\mathbf{z})}{\sqrt{3}}$ and $\mathbf{e}_b=-\mathbf{z}$ in Eq. (1). Our simulations are thus consistent with the experimental finding (observed for thicker PZT films) that changing the growth direction can alter the ground state of thin films.[13]

For *epitaxial* strains and perfect SC conditions, **P** is also given by Eq. (1) and rule 1, but in which λ_1 and λ_2 have to be modified with respect to the corresponding stress-free and SC case, because tensile strain disfavors out-of-plane components of the dipoles while compressive strain favors them.[25,26] Applying a strain in $Pb(Zr_{0.4}Ti_{0.6})O_3$ thin films thus alters the *magnitude* of the polarization when the growth direction is along [001] while it modifies the polarization's *direction* for [110] and [111] films within the monoclinic M_C and M_A phases, respectively, as emphasized by Table I, which displays, for perfect SC conditions, the θ_1 angle between **P** and the growth direction and the θ_2 angle between **P** and $\mathbf{e}_b$. Table I also shows the out-of-plane ϵ_{33} and in-plane $(\epsilon_{11}+\epsilon_{22})/2$ dielectric coefficients computed in the $x'y'z'$ coordinate system, following the correlation-function approach of Ref. 27 (which is only valid for perfect SC conditions). This table reveals that the farther away **P** is from a (bulk) $\langle 001\rangle$ direction, the larger dielectric responses are, which is in agreement with Ref. 13. For instance, going from a stress-free [001] to a compressed [111] film, under ideal SC and at 10 K, results in a rotation of **P** by 18.5° with respect to $\mathbf{e}_b$ and $\simeq$ *triples* the in-plane dielectric coefficients. Note that the compressively strained [111] film has a larger θ_2, and thus larger dielectric response, than the compressively strained [110] film because [111] is farther away from the closest $\langle 001\rangle$ direction than [110] is.

B. Films under small residual depolarizing field: Rule 1

For electrical boundary conditions slightly away from ideal SC conditions, the films continue to follow Eq. (1) and rule 1, but with λ_1 and λ_2 being dependent on β, which reflects the decrease of the out-of-plane component of the polarization in response to the activation of a small depolarizing field. As a result, decreasing β leads to (i) a decrease of the polarization *magnitude* when the growth direction also corresponds to a possible direction for the bulk polarization—i.e., for [001] $Pb(Zr_{0.4}Ti_{0.6})O_3$ [see Figs. 1(a)–1(c)]—*versus* (ii) a *rotation* of the polarization away from $\mathbf{e}_g$ for the other cases [see Figs. 1(d)–1(i)].

At some critical value of the depolarizing field, the films cannot sustain any out-of-plane polarization component anymore and a phase transition occurs. Rule 2 now applies for depolarizing fields larger than this critical field or, equivalently, for the smallest β values.

C. Stress-free films under large residual depolarizing fields: Rule 2

As indicated by Fig. 1(a), the stress-free [001] $Pb(Zr_{0.4}Ti_{0.6})O_3$ film exhibits dipoles that all point along [100]. In order to satisfy rule 2, this film thus adopts a polarization lying along a direction that is a possible direction of the polarization in the bulk and that is *perpendicular* to the growth direction. There is a second way to satisfy rule 2, as followed by the stress-free $Pb(Zr_{0.4}Ti_{0.6})O_3$ films grown along [110] and [111]: the supercell average of the out-of-plane polarization component in these two cases is still equal to zero as in [001] $Pb(Zr_{0.4}Ti_{0.6})O_3$, but [as indicated in the left schematizations above in Figs. 1(d) and 1(e)] this annihilation occurs by developing $\simeq$90° periodic nanostripe domains. (Note that the average angle made by the dipoles belonging to different stripes is in fact close to 70°.) The dipoles inside each domain are aligned along directions that are close to [100] or [010] (which are possible directions for the bulk polarization). The reason behind the dramatic difference in the homogeneity of the dipole patterns between the [111] and [001] films is that all possible $\langle 001\rangle$ directions of the bulk polarization are far away from the planes perpendicular to the growth direction in the case of the [111] film. An homogeneously in-plane polarized [111] film would thus require a significant deviation of the direction of the dipoles with respect to a possible direction of the bulk polarization. Such significant deviation does not occur in stress-free $Pb(Zr_{0.4}Ti_{0.6})O_3$ because of its large anisotropy. On the other hand, the dipoles in the [110] film do have the possibility to all lie along an *in-plane* direction that is also a direction for the bulk: namely, [001]. However, the analysis of our computations reveals that the [110] stress-free film prefers to rather form $\simeq$90° nanostripe domains because of a gain in short-range interactions. Interestingly, 90° periodic stripe do-

mains were previously observed in [111] PZT films,[15] but *not yet* in [110] ferroelectric films, to the best of our knowledge.

D. Films under tensile strain and large residual depolarizing fields: Rule 2

A tensile strain and OC-like conditions both disfavor out-of-plane components of dipoles, because of the strain-dipole coupling and the existence of a large depolarizing field along the growth direction, respectively. As a result, most of the films develop *homogeneous* in-plane polarization pattern [see left schematizations above in Figs. 1(b) and 1(e)]. The only exception from this trend is the [111] $Pb(Zr_{0.4}Ti_{0.6})O_3$ film, as seen in Fig. 1(h). Such an exception is once again caused by the material desire to have dipoles close to the possible polarization directions of the bulk.

E. Films under compressive strain and large residual depolarizing fields: Rule 2

As indicated by the left schematizations above in Figs. 1(c), 1(f), and 1(i), the thin films all adopt flux-closure *periodic nanostripe domains* (which resemble those observed in magnetic films[28–30]) for compressive strains and large residual depolarizing fields because of the competition between the compressive strain that favors out-of-plane components of the dipoles and the large depolarizing field that desires to destroy the out-of-plane component of the polarization.[5,7] Interestingly, the morphology of the stripe domains depends on the growth direction: [001] $Pb(Zr_{0.4}Ti_{0.6})O_3$ exhibits the out-of-plane 180° nanostripes that were observed[5] in [001] $PbTiO_3$ ultrathin films under similar boundary conditions. On the other hand, [110] and [111] $Pb(Zr_{0.4}Ti_{0.6})O_3$ films are more reluctant to have dipoles along the growth directions and prefer to adopt ≃90° nanodomains. (Note that the average angle made by the dipoles belonging to different stripes is in fact close to 105°.) The existence of these latter domains for compressive strain can be traced back to the difficulty of rotating the polarization away from a ⟨100⟩ direction in the $Pb(Zr_{0.4}Ti_{0.6})O_3$ bulk, as demonstrated by the fact that it is possible to transform these ≃90° domains into 180° out-of-plane nanostripe domains in thin films grown along [110] or [111] and having compositions associated with a tetragonal phase in the bulk via two different processes: (1) increase the magnitude of the compressive strain—as we numerically found out in $Pb(Zr_{0.4}Ti_{0.6})O_3$—or (2) decrease the composition towards the morphotropic phase boundary of PZT bulk—i.e., making the polarization easier to rotate—as we numerically checked when going from $Pb(Zr_{0.4}Ti_{0.6})O_3$ to $Pb(Zr_{0.5}Ti_{0.5})O_3$.

F. Equilibrium domain widths

The equilibrium width of the stripe domains is found by varying the in-plane supercell sizes and is given in Å in Fig. 1. The predicted equilibrium domain width of ≃24 Å for the compressed [001] film (having a thickness of 48 Å) is in excellent agreement with the experimental data of Ref. 5 for $PbTiO_3$ ultrathin films having similar thickness and growth orientation. The domain width of ≃22 Å we found for the stress-free and tensile [111] 46.2-Å-thick films agrees also very well with the interpolation, via the well-known square root dependence on the film thickness,[31] of the experimental data of Ref. 15 down to a thickness of ≃46 Å. Specifically, such interpolation results in a domain width of ≃21 Å. We are not aware of any measurements done in stress-free [110], compressed [110], or compressed [111] ultrathin films, for which we predict a domain width of ≃17 Å, 22 Å, and 29 Å, respectively, when these films have a thickness around ≃46–48 Å.

G. Size dependence of the properties

We also determined how *size* affects the properties of stress-free films under SC conditions, by investigating three different ranges of thickness: ≃23–24 Å, ≃46–48 Å, and ≃280 Å. We numerically found that, for any growth orientation, decreasing the film thickness leads to a decrease of ϵ_{33}. Moreover, for the [110] and [111] films, the deviation of **P** from $\mathbf{e}_b$ [see Eq. (1) and rule 1] becomes more pronounced as the thickness of the films decreases. For instance, the angle between **P** and $\mathbf{e}_b$ increases from 1.0° to 9.8° when decreasing the thickness from 280 Å to 23.1 Å in [111] stress-free films at 10 K. The reason behind such a trend is that the ratio between surface and inner layers becomes larger as the thickness decreases while the *surface* layers are the ones exhibiting the *largest* component of the dipoles along the growth direction (because of the lack of the costly short-range interactions outside the films[11]). Our findings are thus also consistent with recent experiments[14] reporting that their *thinnest* [111] $PbZr_{0.35}Ti_{0.65}O_3$ films are *not* tetragonal, unlike their bulk counterpart.

IV. CONCLUSIONS

In summary, we developed and used a first-principles-based approach to reveal that, and understand why, a wide variety of dipole patterns can exist in ultrathin films, depending on the interplay between growth direction and boundary conditions. Examples include the formation of complex nanostripe domains and the occurrence of low-symmetry macroscopic phases that are associated with a direction of the polarization rotating away from that of the bulk. Such growth orientation-induced rotation of polarization can lead to a significant enhancement of dielectric responses.

ACKNOWLEDGMENTS

We thank I. Kornev for useful discussions. This work is supported by NSF Grants Nos. DMR-0404335 and DMR-0080054 (C-SPIN), by ONR Grants Nos. N00014-01-1-0365 (CPD) and N00014-04-1-0413, and by DOE Grant No. DE-FG02-05ER46188.

*Electronic address: iponoma@uark.edu
†Electronic address: laurent@uark.edu

[1] A. V. Bune, Nature (London) **391**, 874 (1998).
[2] T. Tybell, C. H. Ahn, and J.-M. Triscone, Appl. Phys. Lett. **75**, 856 (1999).
[3] Q. Li, J. Yin, C. Xiao, and Z. Liu, J. Phys. D **33**, 107 (2000).
[4] J. Junquera and P. Ghosez, Nature (London) **422**, 506 (2004).
[5] D. Fong, G. Stephenson, S. Streiffer, J. Eastman, O. Auciello, P. Fuoss, and C. Thompson, Science **304**, 1650 (2004).
[6] Z. Wu, N. Huang, Z. Liu, J. Wu, W. Duan, B.-L. Gu, and X.-W. Zhang, Phys. Rev. B **70**, 104108 (2004).
[7] I. Kornev, H. Fu, and L. Bellaiche, Phys. Rev. Lett. **93**, 196104 (2004).
[8] N. Sai, A. M. Kolpak, and A. M. Rappe, Phys. Rev. B **72**, 020101(R) (2005).
[9] C. Lichtensteiger, J. M. Triscone, J. Junquera, and P. Ghosez, Phys. Rev. Lett. **94**, 047603 (2005).
[10] M. Sepliarsky, M. G. Stachiotti, and R. L. Migoni, Phys. Rev. B **72**, 014110 (2005).
[11] P. Ghosez and K. M. Rabe, Appl. Phys. Lett. **76**, 2767 (2000).
[12] Y. Adachi, D. Su, P. Muralt, and N. Setter, Appl. Phys. Lett. **86**, 172904 (2005).
[13] I. Kanno, H. Kotera, T. Matsunaga, T. Kamada, and R. Takayama, J. Appl. Phys. **93**, 4091 (2003).
[14] M. B. Kelman, L. F. Schloss, P. C. McIntyre, B. C. Hendrix, S. M. Bilodeau, and J. F. Roeder, Appl. Phys. Lett. **80**, 1258 (2001).
[15] C. Zybill, B. Li, F. Koch, and T. Graf, Phys. Status Solidi A **177**, 303 (2000).
[16] L. Bellaiche, A. Garcia, and D. Vanderbilt, Phys. Rev. Lett. **84**, 5427 (2000).
[17] B. Noheda, D. E. Cox, G. Shirane, R. Guo, B. Jones, and L. E. Cross, Phys. Rev. B **63**, 014103 (2001).
[18] C.-S. Liang and J.-M. Wu, Appl. Phys. Lett. **87**, 022906 (2005).
[19] T. Maruyama, M. Saitoh, I. Sakai, T. Hidaka, Y. Yano, and T. Noguchi, Appl. Phys. Lett. **73**, 3524 (1998).
[20] L. Bellaiche, A. Garcia, and D. Vanderbilt, Ferroelectrics **266**, 41 (2002).
[21] I. Naumov and H. Fu, cond-mat/0505497 (unpublished).
[22] I. Ponomareva, I. Naumov, I. Kornev, H. Fu, and L. Bellaiche, Phys. Rev. B **72**, 140102(R) (2005).
[23] N. A. Pertsev, V. G. Kukhar, H. Kohlstedt, and R. Waser, Phys. Rev. B **67**, 054107 (2003).
[24] D. Vanderbilt and M. H. Cohen, Phys. Rev. B **63**, 094108 (2001).
[25] W. Zhong, D. Vanderbilt, and K. M. Rabe, Phys. Rev. B **52**, 6301 (1995).
[26] R. E. Cohen, Nature (London) **358**, 136 (1992).
[27] A. Garcia and D. Vanderbilt, in *First-Principles Calculations for Ferroelectrics*, edited by R. E. Cohen (AIP, Woodbury, NY, 1998), Vol. 436, p. 53, note that such method using correlation functions is only valid when no internal fields exists—that is for perfect short-circuit conditions.
[28] J. R. Patel, K. A. Jackson, and J. J. F. Dillon, J. Appl. Phys. **39**, 3767 (1968).
[29] H. Aitlamine, L. Abelmann, and I. B. Puchalska, J. Appl. Phys. **71**, 353 (1991).
[30] A. Hubert and R. Schafer, *Magnetic Domains* (Springer, Berlin, 2000).
[31] C. Kittel, Phys. Rev. **70**, 965 (1946).